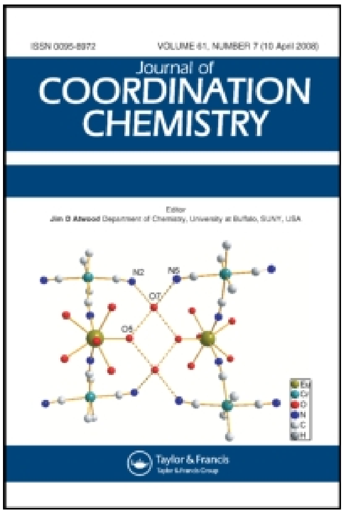

Journal of Coordination Chemistry

Publication details, including instructions for authors and subscription information:
http://www.informaworld.com/smpp/title~content=t713455674

Spectro-thermal characterization of chromium(III) and manganese(II) complexes with carboxyamide

Bibhesh K. Singh[a]; Parshuram Mishra[a]; Bhagwan S. Garg[a]
[a] Department of Chemistry, University of Delhi, Delhi-110007, India

To cite this Article Singh, Bibhesh K. , Mishra, Parshuram and Garg, Bhagwan S.(2008) 'Spectro-thermal characterization of chromium(III) and manganese(II) complexes with carboxyamide', Journal of Coordination Chemistry, 61: 14, 2325 — 2333

To link to this Article: DOI: 10.1080/00958970801907755

URL: http://dx.doi.org/10.1080/00958970801907755

Journal of Coordination Chemistry
Vol. 61, No. 14, 20 July 2008, 2325–2333

Taylor & Francis
Taylor & Francis Group

Spectro-thermal characterization of chromium(III) and manganese(II) complexes with carboxyamide

BIBHESH K. SINGH*, PARSHURAM MISHRA and BHAGWAN S. GARG

Department of Chemistry, University of Delhi, Delhi – 110007, India

(*Received 3 August 2007; in final form 21 September 2007*)

Complexes of Cr(III) and Mn(II) with *N*′,*N*″-bis(3-carboxy-1-oxopropanyl) 2-amino-*N*-arylbenzamidine (H_2L^1) and *N*′,*N*″-*bis*(3-carboxy-1-oxophenelenyl) 2-amino-*N*-arylbenzamidine (H_2L^2) have been synthesized and characterized by various physico-chemical techniques. The vibrational spectral data are in agreement with coordination of amide and carboxylate oxygen of the ligands with the metal ions. The electronic spectra indicate octahedral geometry around the metal ions, supported by magnetic susceptibility measurements. The thermal behavior of chromium(III) complexes shows that uncoordinated nitrate is removed in the first step, followed by two water molecules and then decomposition of the ligand; manganese(II) complexes show two waters removed in the first step, followed by removal of the ligand in subsequent steps. Kinetic and thermodynamic parameters were computed from the thermal data using Coats and Redfern method, which confirm first order kinetics. The thermal stability of metal complexes has been compared. X-ray powder diffraction determines the cell parameters of the complexes.

Keywords: Amide; Metal complexes; Spectra; Thermodynamic activation parameters; X-ray powder diffraction studies

1. Introduction

Interest in transition metal complexes containing amide ligands stems from the fact that such complexes can be easily made and variation of the substituents is facile. These characteristics provide the possibility of tailoring the bite angle and degree of steric hindrance in the ligand. The chemistry of metal complexes containing amidine, a key functional group in a wide range of biologically active molecules [1], including a variety of serine protease inhibitors [1–3] and antimicrobial agents [4], has received a great deal of attention. The structure and mode of bonding of amide aids in the development of amide-metal interactions [5, 6]. Our research is centered on thermal stability and structures of metal complexes of carboxyamides. Though much work has been done on amide ligands in general and amide ligands in combination with other functional groups, less has been done on amide systems containing carboxylic anchors, which may act as biomimics to peptides and certain enzymes. Ligands containing carboxyamide chains having O_4 donor atoms, and their complexes, have been cited as possessing

---

*Corresponding author. Tel.: +91 9410311467. Fax: +91 27666250. Email: bibheshksingh@yahoo.co.in

Journal of Coordination Chemistry
ISSN 0095-8972 print/ISSN 1029-0389 online © 2008 Taylor & Francis
DOI: 10.1080/00958970801907755

pharmacological activity [7]. Thus, we have designed amide ligands containing carboxylic anchors condensed with amidines.

Manganese and its compounds have some medicinal as well as biological importance, playing a significant role in enzyme activation. Citrate cyclase catalyzes the cleavage of citrate to oxaloacetate and acetate in the presence of manganese(II) [8]. Water-soluble chromium(III) compounds are not considered carcinogenic [9], but can form stable biomolecules with amino acids and DNA [10]. In the present manuscript, we report the preparation, spectral characterization and thermal decomposition kinetics of Cr(III) and Mn(II) complexes of the newly synthesized ligands *N′*, *N″-bis*(3-*carboxy*-1-*oxopropanyl*) 2-*amino*-*N*-*arylbenzamidine* and *N′*, *N″-bis*(3-*carboxy*-1-*oxophenelenyl*) 2-*amino*-*N*-*arylbenzamidine*.

2. Experimental

2.1. *Materials and methodology*

All the chemicals used in this study were of analytical grade and used as received. Solvents were of analytical grade and purified by standard procedures. Analyses (C, H and N) of the complexes were performed using Elementar Vario EL III (Germany) model. Metal contents were estimated on an AA-640-13 Shimadzu flame atomic absorption spectrophotometer in solution prepared by decomposing the respective complex in hot concentrated HNO_3. The XRD powder patterns were recorded on a vertical type Philips 1130/00 X-ray diffractometer operated at 40 kV and 50 Ma generator using the Cu-Kα line at 1.54056 Å as the radiation source. The sample was scanned between 5° to 70° (2θ) at 25°C. The crystallographic data were analyzed by using the CRYSFIRE–2000 powder indexing software package and the space group was found by GSAS program. Debye–Scherer relation with the help of 100% peak width determined the particle size. The density was determined by Archimedes method. IR spectra were recorded on a Perkin-Elmer FT-IR spectrophotometer in KBr and polyethylene pellets. The electronic spectra were recorded in water on a Beckman DU-64 spectrophotometer with quartz cells of 1 cm path length. Rigaku model 8150 thermoanalyzer (Thermaflex) was used for simultaneous recording of TG-DTA curves at a heating rate of $10^\circ\,\mathrm{min}^{-1}$. For TG, the instrument was calibrated using calcium oxalate, while for DTA calibration was done using indium metal, both of which were supplied with the instrument. A flat bed type aluminum crucible was used with α-alumina (99% pure) as the reference material for DTA. The number of decomposition steps was identified using TG. The activation energy and Arrhenius constant of the degradation process were obtained by the Coats and Redfern method.

2.2. *Synthesis of complexes*

Synthesis of chromium(III) and manganese(II) complexes of *N′*, *N″-bis*(3-*carboxy*-1-*oxopropanyl*) 2-*amino*-*N*-*arylbenzamidine* (L^1) (complexes **1** and **2**, respectively) and *N′*,*N″-bis*(3-*carboxy*-1-*oxophenelenyl*) 2-*amino*-*N*-*arylbenzamidine* (L^2) (complexes **3** and **4**, respectively).

Table 1. Color, reaction yield and elemental analysis of the complexes.

Compound/ complex	Empirical formula	Color	Yield (%)	Analysis: found (calculated) (%) C	H	N	M
$[Cr(L^1)(H_2O)_2]NO_3$	$C_{21}H_{23}N_4O_{11}Cr$	Green	80	45.00 (45.09)	4.05 (4.14)	10.00 (10.01)	9.22 (9.29)
$[Mn(L^1)(H_2O)_2]$	$C_{21}H_{23}N_3O_8Mn$	Pale pink	78	50.36 (50.41)	4.55 (4.63)	8.37 (8.40)	10.92 (10.98)
$[Cr(L^2)(H_2O)_2]NO_3$	$C_{29}H_{23}N_4O_{11}Cr$	Dark green	81	53.09 (53.14)	3.49 (3.54)	8.51 (8.55)	7.88 (7.93)
$[Mn(L^2)(H_2O)_2]$	$C_{29}H_{23}N_3O_8Mn$	Pale pink	77	58.31 (58.40)	3.83 (3.89)	7.01 (7.05)	9.16 (9.21)

The syntheses and characterization of L^1 and L^2 were reported recently [11]. To a methanolic solution of $Cr(NO_3)_3 \cdot 9H_2O$ and $Mn(CH_3CO_2)_2 \cdot 4H_2O$ (0.5 mmol) each in a separate flask were added a methanolic solution of the ligands (L^1) and (L^2) (0.5 mmol). The solution was stirred for 3 h, after which the volume was reduced on a warm water bath. The product obtained was washed with a small amount of methanol and air–dried. The product was redissolved in excess warm methanol, and clear solution was left undisturbed for weeks to give colored crystals of the complexes.

3. Results and discussion

Satisfactory elemental analyses (table 1) and spectral studies revealed that the ligands and complexes were of good purity. The complexes were soluble in polar solvents. The general chemical reaction for the complex formation is

$$Cr(NO_3) \cdot 9H_2O + H_2L \rightarrow [Cr(L)(H_2O)_2](NO_3) + 7H_2O + 2HNO_3$$

$$Mn(CH_3COO)_2 \cdot 4H_2O + H_2L \rightarrow [Mn(L)(H_2O)_2] + 2H_2O + 2CH_3COOH$$

where $L{=}L^1$ and L^2.

3.1. *Spectral characterization and magnetic studies*

The ambidentate amide can coordinate with chromium(III) and manganese(II) either through nitrogen of the $-NH_2$ or oxygen of the C=O. Bands due to amide ν(N–H) at 3200–3400 cm^{-1} for the free ligands L^1 and L^2 are shifted to higher frequencies, while the ν(C=O) (amide I) frequency (1630–1650 cm^{-1}) undergoes shift to lower frequency (1600–1640 cm^{-1}) in the metal complexes indicating non–involvement of the amide nitrogen and involvement of the carbonyl oxygen atom of amide group in coordination with the metal [12] (supplemental material). This result is explained by decrease in the double bond character of C=O and the subsequent increase of C–N double bond character [13, 14]. Amide II (1410–1480 cm^{-1} in ligands) and Amide III (1275–1305 cm^{-1} in ligands) arising from ν(C–N) as well as δ(N–H) modes (coupled to one another), shift to higher frequencies 1430–1530 cm^{-1} and 1295–1340 cm^{-1}, respectively in complexes further confirming coordination through carbonyl oxygen. The ν(C=O) and ν(C–O) stretching frequencies in the 1540–1590 cm^{-1} and 1420–1400 cm^{-1} region in the uncomplexed ligands have been assigned to $\nu_{as}(CO_2^-)$ and $\nu_s(CO_2^-)$ modes of the carboxylate group and these bands show considerable shift

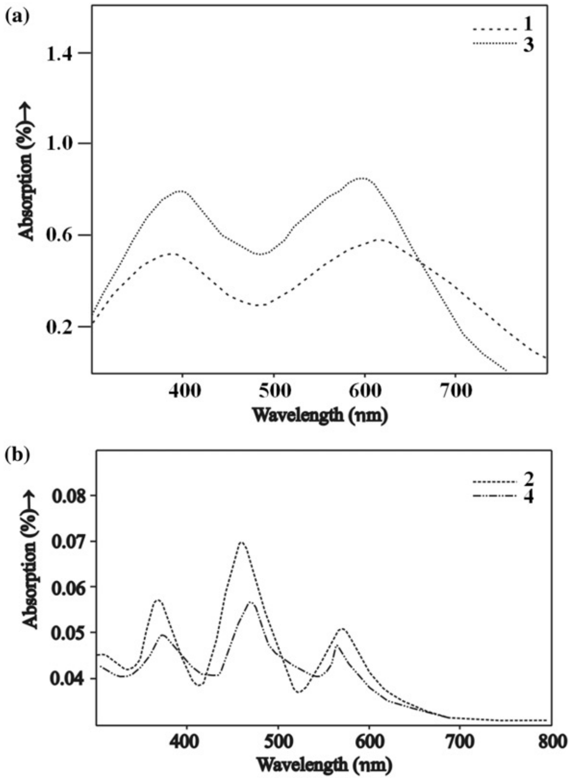

Figure 1. (a) Electronic spectra of complexes **1** and **3**; (b) Electronic spectra of complexes **2** and **4**.

in the complexes. A positive and negative shift indicates a $\Delta\nu$ enhancement upon complexation and suggests monodentate coordination of carboxylate in the complexes [15, 16]. Here $\Delta\nu$ implies the difference between $\nu_{as}(CO_2^-)$ and $\nu_s(CO_2^-)$. The ν(O–H) due to carboxylic group at 2600 cm^{-1} in the free ligands disappears in the spectra of complexes, indicating both carboxylates are involved in complexation. The vibrational bands due to rocking and wagging modes of water are observed in the 800–350 cm^{-1} region, attributed to coordinated water in all the complexes [15]. This is confirmed by thermograms. In the spectra of chromium complexes, a sharp strong band at 1385–1384 cm^{-1} confirms the presence of uncoordinated nitrate [17]. A new band at 625–335 cm^{-1} is assigned to ν(M–O) [18].

Electronic spectra of the ligands and complexes have been studied in the range 190–900 nm. The shoulder at 279 nm in water for ligands may be assigned to $n \rightarrow n^*$ transition within the C=O group of the amide. This band disappears in all the complexes, revealing involvement of the C=O of amide group or carboxylate in chelate formation. The bands at 328 and 318 nm in L^1 and L^2 may be assigned to $\pi \rightarrow \pi^*$ of the N-amino group of the amide ligand, unchanged in the metal complexes, indicating they are not affected by metal chelation [19]. In the visible region, chromium complexes (figure 1a) have three absorption bands, 16393–17240 cm^{-1}, 24390–25640 cm^{-1} and 19800–20200 cm^{-1} (as a shoulder), assigned to $^4A_{2g} \rightarrow {}^4T_{2g}(F)$, $^4A_{2g} \rightarrow {}^4T_{1g}(F)$, and the last band is very weak, belonging to a forbidden band

Table 2. Thermoanalytical data (TG, DTA) of the metal complexes.

Complex	Step	T_g range/K	DTA$_{max}$/K	Thermal effect	Mass loss obs (Calcd)%	Assignment	Metallic residue
	I	318–358	342	Endo	11.00(11.58)	$NO_2+½O_2$	
$[Cr(L^1)(H_2O)_2]NO_3$	II	390–432	418	Endo	6.40(6.44)	$2H_2O$	Cr_2O_3
	III	623–823	683	Exo	55.60(55.31)	Organic moiety	
	I	363–423	390	Endo	7.20(7.19)	$2H_2O$	MnO
$[Mn(L^1)(H_2O)_2]$	II	475–875	633	Exo	78.60(78.62)	Organic moiety	
	I	320–360	338	Endo	10.00(9.46)	$NO_2+½O_2$	Cr_2O_3
$Cr(L^2)(H_2O)_2]NO_3$	II	393–438	419	Endo	5.50(5.49)	$2H_2O$	
	III	573–876	701	Exo	76.80(76.81)	Organic moiety	
	I	368–443	399	Endo	6.00(6.04)	$2H_2O$	MnO
$[Mn(L^2)(H_2O)_2]$	II	573–773	663	Exo	82.00(82.06)	Organic moiety	

$^4A_{2g} \rightarrow {}^2E_g(G)$. The 10$D_q$ energy of **1** was calculated from the Tanabe-Sugano diagrams as 16670 cm^{-1}. The observed magnetic moments of chromium(III) complexes are in the range of 4.20–4.35 BM supporting octahedral structures. The electronic spectra of Mn(II) complexes (figure 1b) exhibit four weak intensity absorption bands 18410–19500 cm^{-1}, 22725–23525 cm^{-1}, 28010–28490 cm^{-1} and 38460–38610 cm^{-1}. These bands may be assigned to $^6A_{1g} \rightarrow {}^4T_{1g}(^4G)$, $^6A_{1g} \rightarrow {}^4E_g$, $^4A_{1g}(^4G)$, $^6A_{1g} \rightarrow {}^4E_g(^4D)$, and $^6A_{1g} \rightarrow {}^4T_{1g}(^4P)$, respectively, in the range reported for octahedral Mn(II) [20]. The magnetic moments (5.30–5.50 BM) are additional evidence for an octahedral manganese(II).

3.2. *Thermoanalytical studies*

Rate-dependent parameters of solid-state non-isothermal decomposition reactions can be obtained by analysis of TG curves [21–23]. Thermogravimetric (TG) and differential thermogravimetric (DTA) analyses were carried out for the complexes in ambient conditions (supplemental material). The correlations between the different decomposition steps of the complexes with the corresponding weight losses are summarized in table 2. The final product of decomposition corresponds to metal oxide, confirmed by comparing the observed/estimated and the calculated mass of the pyrolysis product.

3.3. *Kinetics of thermal decomposition*

Several equations [24–30] have been proposed to analyze a TG curve and obtain kinetic parameters. Many authors [24–28] have discussed the advantage of this method over the conventional isothermal method. Most commonly used methods are the differential method of Freeman and Carroll [24], integral method of Coats and Redfern [26], and the approximation method of Horowitz and Metzger [29]. The kinetic parameters calculated by the Horowitz–Metzger method revealed no significant difference with that evaluated by the Coats–Redfern method.

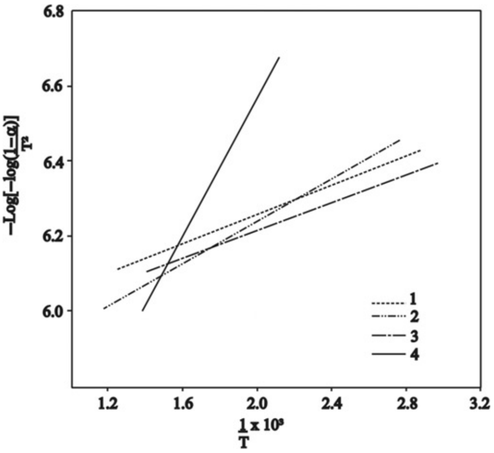

Figure 2. Coats & Redfern linearization plot of complexes **1**–**4**.

Table 3. Thermodynamic activation parameters of the complexes.

Complex	Order/*n*	Steps	E^* (J mol^{-1})	A (s^{-1})	ΔS^* (JK^{-1} mol^{-1})	ΔH^* (J mol^{-1})	ΔG^* (kJ mol^{-1})
$[Cr(L^1)(H_2O)_2]NO_3$	1	I	90.79	2.04×10^6	−125.05	32.68	42.80
		II	95.56	1.84×10^6	−127.57	24.35	53.35
		III	72.63	6.46×10^5	−140.34	102.56	95.95
$[Mn(L^1)(H_2O)_2]$	1	I	70.99	8.43×10^5	−133.48	26.72	52.08
		II	60.07	3.70×10^5	−144.33	89.16	91.45
$Cr((L^2)(H_2O)_2]NO_3$	1	I	95.57	2.18×10^6	−124.40	13.23	42.06
		II	101.94	2.00×10^6	−126.90	34.97	53.21
		III	95.57	1.04×10^6	−136.60	179.22	95.94
$[Mn((L^2)(H_2O)_2]$	1	I	20.24	3.33×10^4	−160.49	26.65	64.06
		II	21.02	2.16×10^4	−168.30	82.70	111.67

The kinetic analysis parameters such as activation energy (ΔE^*), enthalpy of activation (ΔH^*), entropy of activation (ΔS^*), and free energy change of decomposition (ΔG^*) were evaluated graphically by employing the Coats–Redfern relation (1)

$$\log\left[-\log\left(\frac{1-\alpha}{T^2}\right)\right] = \frac{\log[\mathrm{AR}/\theta\, E^*(1-2\mathrm{R}T/E^*)] - E^*}{2.303\ \mathrm{R}T} \tag{1}$$

where α is the mass loss up to the temperature T, R is the gas constant, E^* is the activation energy in J mol^{-1}, θ is the linear heating rate and $(1 - 2\mathrm{R}T/\mathrm{E}^*) \cong 1$. A plot of the left hand side of equation (1) against $1/T$ gives a slope from which E^* was calculated and A (Arrhenius constant) was determined from the intercept. From relevant data, linearization plots have been drawn in figure 2 confirming first order kinetics. The entropy of activation (ΔS^*) and the free energy change of activation (ΔG^*) were calculated using equations (2) and (3).

$$\Delta \mathrm{S}^* = 2.303\mathrm{R}\left[\log\left(\frac{\mathrm{Ah}}{kT}\right)\right]\mathrm{JK}^{-1}\,\mathrm{mol}^{-1} \tag{2}$$

$$\Delta G^* = \Delta \mathrm{H}^* - T\Delta \mathrm{S}^* \mathrm{J\ mol}^{-1} \tag{3}$$

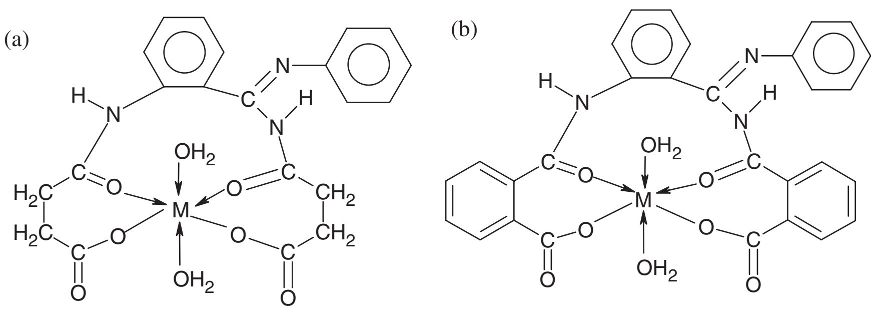

Complex **1**: M = Cr(III) NO_3
Complex **2**: M = Mn(II)

Complex **3**: M = Cr(III) NO_3
Complex **4**: M = Mn(II)

Figure 3. Proposed structures of the complexes (a) Complex **1**: M=Cr(III) NO_3 Complex **2**: M=Mn(II); (b) Complex **3**: M=Cr(III) NO_3 Complex **4**: M=Mn(II).

Table 4. Crystallographic data of the complexes.

Empirical formula	$C_{21}H_{23}N_4O_{11}Cr$ (Complex **1**)	$C_{29}H_{23}N_4O_{11}Cr$ (Complex **3**)	$C_{29}H_{23}N_3O_8Mn$ (Complex **4**)
Formula weight	559.42	655.51	596.45
Temperature (K)	298	298	298
Wavelength (Å)	1.54056	1.54056	1.54056
Crystal system	Monoclinic	Tetragonal	Tetragonal
Space group	$P_{2/m}$	$P_{4/m}$	$P_{4/m}$
Unit cell dimensions (Å, °)			
a	13.921880	15.527190	14.767020
b	12.756270	15.527190	7.036438
c	7.759273	11.654910	4.536596
α	90	90	90
β	113.9110	90	90
γ	90	90	90
Volume (Å^3)	628.12	1840.69	533.44
2θ range (°)	10–70	10–70	10–70
Limiting indices	$-7 \leq h \leq 6$	$0 \leq h \leq 7$	$0 \leq h \leq 3$
	$0 \leq k \leq 7$	$0 \leq k \leq 6$	$0 \leq k \leq 3$
	$0 \leq l \leq 3$	$0 \leq l \leq 4$	$0 \leq l \leq 4$
Density (g cc^{-1})	1.396	1.182	1.856
Z	2	2	1
Avs. Eps	0.0000488	0.0001075	0.0001183
Reflections	1116	1442	4884
Particle size (nm)	8.591	9.550	6.136
R_f	0.0025	0.0025	0.0025
Merit of fit	$M(14) = 6$, $F(14) = 3$	$M(8) = 6$, $F(8) = 3$	$M(7) = 15$, $F(7) = 4$

where k and h are the Boltzman and Plank constant, respectively. The calculated values of E^*, A, ΔS^*, ΔH^* and ΔG^* for the decomposition steps of the complexes are given in table 3. According to the kinetic data obtained from TG curves, the activation energy relates the thermal stability of the metal complexes. Activation energy increases as $\mathbf{4} < \mathbf{2} < \mathbf{1} < \mathbf{3}$. All the complexes have negative entropy, indicating a more ordered activated state that may be possible through chemisorption of oxygen and other decomposition products. The negative values of the entropies of activation are compensated by the values of the enthalpies of activation, leading to almost the same values for the free energy of activation [31].

3.4. *X-ray powder diffraction studies*

In the absence of single crystals, X-ray powder data are useful to deduce cell parameters. The diffraction pattern reveals the crystalline nature of the complex. The indexing procedures were performed using (CCP_4, UK) Crysfire [32] giving different crystal system with varying space group. The merit of fit and particle size of the metal complexes have been calculated (supplemental data, XRPD spectra of complexes **3** and **4**). The cell parameters of the complexes are shown in table 4.

4. Conclusions

Metal complexes were mononuclear and coordinated through carboxylate oxygen of the amide ligands as revealed by IR. Vibrational spectra indicate the presence of H_2O in the complexes, supported by TG/DTA. Chromium(III) complexes contain uncoordinated nitrate. Kinetic parameters show that decomposition follows first order kinetics and proceeds in two/three-step decomposition. Thermal stabilities of the complexes have been compared. The electronic spectra indicate octahedral geometry around the metal ions, supported by magnetic studies. The complex crystallizes in the monoclinic/tetragonal crystal system.

Acknowledgement

B.K. Singh is thankful to the University Grants Commission, New Delhi, India, for financial assistance under research award scheme.

References

[1] J.V. Greenhill, P. Lue. *Prog. Med. Chem.*, **30**, 203 (1993).
[2] M.J. Rudolph, CR. Illig, N.L. Subasinghe, K.J. Wilson, J.B. Hoffman, T. Randle, D. Green, C.J. Molloy, R.M. Soll, F. Lewandowski, M. Zhang, R. Bone, J.C. Spurlino, I.C. Deckman, C. Manthey, C. Sharp, D. Maguire, B.L. Grasberger, R.L. DesJarlais, Z. Zhou. *Bioorg. Med. Chem. Lett.*, **12**, 491 (2002).
[3] J.M. Fevig, D.H. Pinto, Q. Han, M.L. Quan, J.R. Pruitt, I.C. Jacobson, R.A. Galemmo Jr, S. Wang, M.J. Orwat, L.L. Bostrom, R.M. Knabb, P.C. Wong, P.Y.S. Lam, R.R. Wexler. *Bioorg. Med. Chem. Lett.* **11**, 641 (2001).
[4] R.R. Tidwell, D.W. Boykin. Dicationic DNA Minor Groover Binders as Antimicrobial Agents. In *Small Molecule DNA and RNA Binders: From Synthesis to Nucleic Acid Complexes*, M. Demeunynch, C. Bailly, W.D. Wilson (Eds.), Vol. 2, pp. 416–460, Wiley-VCH, New York (2003).
[5] B.S. Garg, D.N. Kumar, M. Sarbhai. *Spectrochim. Acta A*, **61**, 141 (2005).
[6] B.S. Garg, R.K. Sharma, V. Kumar, M.J. Reddy, S. Mittal. *Spectrochim. Acta A*, **58**, 2789 (2002).
[7] B.S. Garg, M. Sarbhai, D.N. Kumar. *Ind. J. Chem.*, **42A**, 275 (2003).
[8] H. Sigel (Ed.). *Metal Ions in Biological Systems*, Vol. 13, p. 181, Marcel Dekker, New York (2002).
[9] *IARC Monograph on the Evaluation of Carcinogenic Risk to Humans, Chromium, Nickel & Welding*, Vol. 48, pp. 49–508, IARC, Lyon, France (1990).
[10] A. Zhitkovich, V. Voitkun, M. Costa. *Biochemistry*, **35**, 7275 (1996).
[11] B.K. Singh, P. Mishra, B.S. Garg. *Trans. Met. Chem.*, **32**, 603 (2007).
[12] T.A. Kabanos, J.M. Tsangaris. *J. Coord. Chem.*, **13**, 89 (1984).
[13] M. Nonoyama, K. Yamasaki. *Inorg. Chim. Acta*, **3**, 585 (1969).

[14] D.J. Barnes, R.L. Chapman, F.S. Stephens, R.S. Vagg. *Inorg. Chim. Acta*, **51**, 155 (1981).
[15] K. Nakamoto. *Infrared and Raman Spectra of Inorganic and Coordination Compounds*, 3rd Edn, Wiley, New York (1978).
[16] T. Sarojini, A. Ramachandrraiah. *Ind. J. Chem.*, **29A**, 1174 (1990).
[17] M. Tiliakos, P. Cordopatis, A. Terzis, C.P. Raptopoulou, S.P. Perlepes, E. Manessi–Zoupa. *Polyhedron*, **20**, 2203 (2001).
[18] F.F. Bentley, L.D. Smithson, A.L. Rozek. *Infrared Spectra and Characteristic Frequencies* ~*700–300 cm*$^{-1}$, Interscience Publishers, New York (1968).
[19] M.M. Abd–Elzaher. *J. Chin. Chem. Soc.*, **48**, 153 (2001).
[20] F.A. Cotton, G. Wilkinson. *Advanced Inorganic Chemistry*, 3rd US Edn, Wiley, New York (1972).
[21] B.K. Singh, R.K. Sharma, B.S. Garg. *J. Therm. Anal. Calorim.*, **84**, 593 (2006).
[22] B.K. Singh, R.K. Sharma, B.S. Garg. *Main Group Chem.*, **4**(4), 247 (2005).
[23] B.K. Singh, B.S. Garg. *J. Ind. Chem. Soc.*, **82**, 1191 (2005).
[24] E.S. Freeman, B. Carroll. *J. Phys. Chem.*, **62**, 394 (1958).
[25] J. Sestak, V. Satava, W. Wendlandt. *Thermochim. Acta*, **7**, 333 (1973).
[26] A.W. Coats, J.P. Redfern. *Nature*, **68**, 201 (1964).
[27] T. Ozawa. *Bull. Chem. Soc. Jpn.*, **38**, 1881 (1965).
[28] W.W. Wendlandt. *Thermal Methods of Analysis*, Wiley, New York (1974).
[29] H.W. Horowitz, G. Metzger. *Anal. Chem.*, **35**, 1464 (1963).
[30] J.H. Flynn, A. Wall. *Polym. Lett.*, **4**, 323 (1966).
[31] B.K. Singh, R.K. Sharma, B.S. Garg. *Spectrochim. Acta A*, **63**, 96 (2006).
[32] R. Shirley. *The CRYSFIRE System for Automatic Powder Indexing*: Users manual (Lattice Press) (2002).